Dalton Transactions

ROYAL SOCIETY OF CHEMISTRY

PAPER

View Article Online
View Journal | View Issue



Cite this: *Dalton Trans.*, 2022, **51**, 17216

# Assessing the donor ability of boratabenzene and 9-borataphenanthrene anions through metal complexes with carbonyl ligands†

Katherine Rojales,‡ Masilamani Tamizmani,‡ Tyler A. Bartholome and Caleb D. Martin *

Received 26th August 2022,
Accepted 19th October 2022

DOI: 10.1039/d2dt02795j

rsc.li/dalton

A series of anionic group 6 tricarbonyl and neutral rhodium dicarbonyl complexes featuring a boratabenzene (**L1**, with a phenyl on boron, a trimethylsilyl group on the adjacent carbon and methyl groups on the other carbons) and a borataphenanthrene ligand (**L2**, with a phenyl group on boron and a trimethylsilyl group on the adjacent carbon) are prepared. The donor ability of the boracyclic ligands is evaluated experimentally and theoretically by the stretching frequencies of the CO ancillary ligands. Overall, the donor ability of the ligands falls into the following trend: **L1** > cyclopentadienyl > **L2** > mesitylene.



## Introduction

Boratabenzene metal complexes have been known for half a century from the work of Herberich and coworkers in which a borylene unit was formally inserted into a cyclopentadienide (Cp) ligand of cobaltocene.[1] Comparisons of boratabenzene can be drawn to the hydrocarbon ligands benzene and cyclopentadienide due to the six-membered ring and monoanionic charge, respectively.[2] Cyclopentadienide is a better electron donor than benzene as a result of the coulombic attraction of the anionic ligand to electropositive metals.[3] Boratabenzene transition metal complexes have been reported to be efficient catalysts for olefin polymerization, alkene hydrogenation, and cyclotrimerization reactions and are useful in promoting asymmetric reactions while lanthanide complexes can exhibit single-ion magnetic properties.[4]

Carbonyl ligands are effective indicators for the donor strength of ancillary ligands due to their diagnostic infrared signatures as the electron density at metal centers is correlated to the π-backbonding to the π-acidic carbonyls.[5] Such π-backbonding is well studied with arene ligands and cyclopentadienide ligands but less with boratabenzene species.[6] In 1983, Herberich *et al.* reported the methyl-substituted boratabenzene chromium complex (**A**, Fig. 1) and remarked that the CO stretching frequencies were lower than in the corresponding arene analogues (benzene and mesitylene), consistent with greater π-backbonding.[7] Fontaine and coworkers generated an analogous boratabenzene chromium piano-stool complex with a chloride on boron and a trimethylsilyl (TMS) group on one of the adjacent carbons in solution; however, evaporation of the volatiles led to the isolation of a bimetallic inverse sandwich complex (**B**).[8] These bimetallic inverse sandwich chromium complexes do not occur with benzene or cyclopentadienide, indicating that boratabenzenes have different reactivity from the carbonaceous species.[6c,d,9]

In this work, we synthesize and evaluate the full complement of a substituted boratabenzene, and the recently reported substituted tricyclic variant, 9-borataphenanthrene,[10] group 6 anionic metal complexes with three carbonyl ligands completing the coordination sphere to evaluate the donor ability of the boracyclic anionic ligands. The boratabenzene ligand selected features a phenyl group on boron, a trimethylsilyl group on the adjacent carbon, and four methyl groups on the remaining ring carbons (**L1**) while the borataphenanthrene has a biphenyl unit in place of the four methyl groups (**L2**),

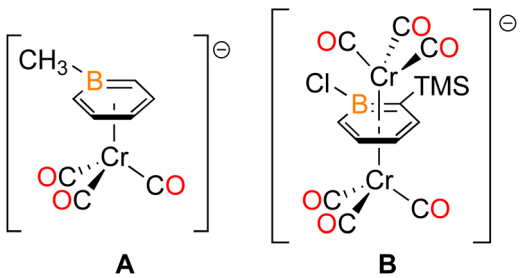


**Fig. 1** Known boratabenzene group 6 metal carbonyl complexes.

*Baylor University, Department of Chemistry and Biochemistry, One Bear Place #97348, Waco, TX, 76798, USA. E-mail: caleb_d_martin@baylor.edu*

†Electronic supplementary information (ESI) available: Multinuclear NMR spectra, FT-IR spectra, X-ray crystallographic table, and computational details. CCDC 2203739–2203745. For ESI and crystallographic data in CIF or other electronic format see DOI: https://doi.org/10.1039/d2dt02795j

‡Equal contribution.

with both generated from anti-aromatic borole precursors.[10,11] The group 6 metal complexes are anionic, and it is known that counter cations can influence the IR stretching frequencies.[6a] Accordingly, we prepared neutral Rh(I) complexes with two carbonyl ligands to circumvent cation effects.

## Results and discussion

The reactions of boracyclic ligands **L1** and **L2** with $(MeCN)_3M(CO)_3$ reagents (M = Cr, Mo, W for **L1**; M = Mo, W for **L2**) were conducted at 23 °C and furnished the corresponding metal complexes **1Cr**, **1Mo**, **1W**, **2Mo**, and **2W**, respectively (Scheme 1). This methodology was based on the recently reported synthetic route to access **2Cr**.[10] In the reactions with **L1** the disappearance of the singlet at 37.4 ppm in the *in situ* $^{11}B$ NMR spectra was observed along with the emergence of singlets further upfield at $\delta$ 27.0 ppm (**1Cr**), $\delta$ 29.5 ppm (**1Mo**), and 28.5 ppm (**1W**) with complete consumption of **L1** within 2 hours. The potassium counter-cations were sequestered with 18-crown-6, leading to the isolation of the products in 41% (**1Cr**), 78% (**1Mo**), and 26% (**1W**) yields. The $^{13}C\{^1H\}$ NMR spectra show carbonyl singlets at $\delta$ 241.9 ppm (**1Cr**), 232.4 ppm (**1Mo**), and 223.4 ppm (**1W**). The $^1H$ NMR spectrum of **1Cr** and **1Mo** in $CD_3CN$ show broad signals for the phenyl protons at room temperature which are resolved at 10 °C for both which may be attributed to rotation about the B–Ph bond.

Similarly, the corresponding reactions of **L2** were complete within 2 hours as indicated by *in situ* $^{11}B$ NMR spectroscopy with the disappearance of the signal at 40.4 ppm for **L2** and emergence of singlets at 33.2 ppm (**2Mo**) and 30.8 ppm (**2W**). Chelation of the potassium counter-cation with dibenzo-18-crown-6 enabled isolation in 67% (**2Mo**) and 48% yields (**2W**). The carbonyl resonances in the $^{13}C\{^1H\}$ NMR spectra appeared at 228.8 ppm (**2Mo**) and 218.6 ppm (**2W**). The identity of all five complexes was confirmed by single crystal X-ray diffraction studies revealing $\eta^6$ coordination of the $BC_5$ rings to the metal centers (Fig. 2).

Given that cations can affect CO stretching frequencies *via* coordination to the oxygen atoms, we synthesized charge-neutral rhodium piano-stool complexes **1Rh** and **2Rh** by treatment of the ligands **L1** and **L2**, respectively, with $Rh_2Cl_2(CO)_4$ in THF at 23 °C (Scheme 2). The reactions were complete within 45 minutes and the resulting rhodium dicarbonyl products were isolated in 81% (**1Rh**) and 88% (**2Rh**) yields. The $^{11}B$ NMR resonances at 26.1 and 35.1 ppm are shifted upfield (*cf.* 37.4 ppm for **L1** and 40.4 ppm for **L2**). As in the group 6 complexes with **L1**, the $^1H$ NMR spectrum of **1Rh** in $C_6D_6$ is broad in the phenyl region which sharpens at 10 °C. The single crystal X-ray diffraction structures of complexes **1Rh** and **2Rh** confirm $\eta^6$ coordination of the ligands to the metal center, akin to the group 6 complexes (Fig. 3).

The solid-state structures obtained from single crystal diffraction studies are depicted in Fig. 2 and 3 with the notable bond lengths presented in Table 1. All group 6 complexes have highly planar $BC_5$ rings with the root-mean-square deviation from planarity ranging between 0.021–0.037 Å. The $BC_5$ rings of the rhodium complexes are also planar with slightly higher deviation from planarity of 0.047 Å for **1Rh** and 0.070 Å for **2Rh**. In all group 6 complexes, the M–B bond is notably longer than all of the M–C bonds of the boracycle.[2c] Examining the distance of the centroid of the $BC_5$ ligand to the metal reveals shorter distances to **L1** than **L2** for all four elements with the greatest difference being for molybdenum ($\Delta$ = 0.063 Å) and smallest for chromium ($\Delta$ = 0.053 Å). The average C–O bond

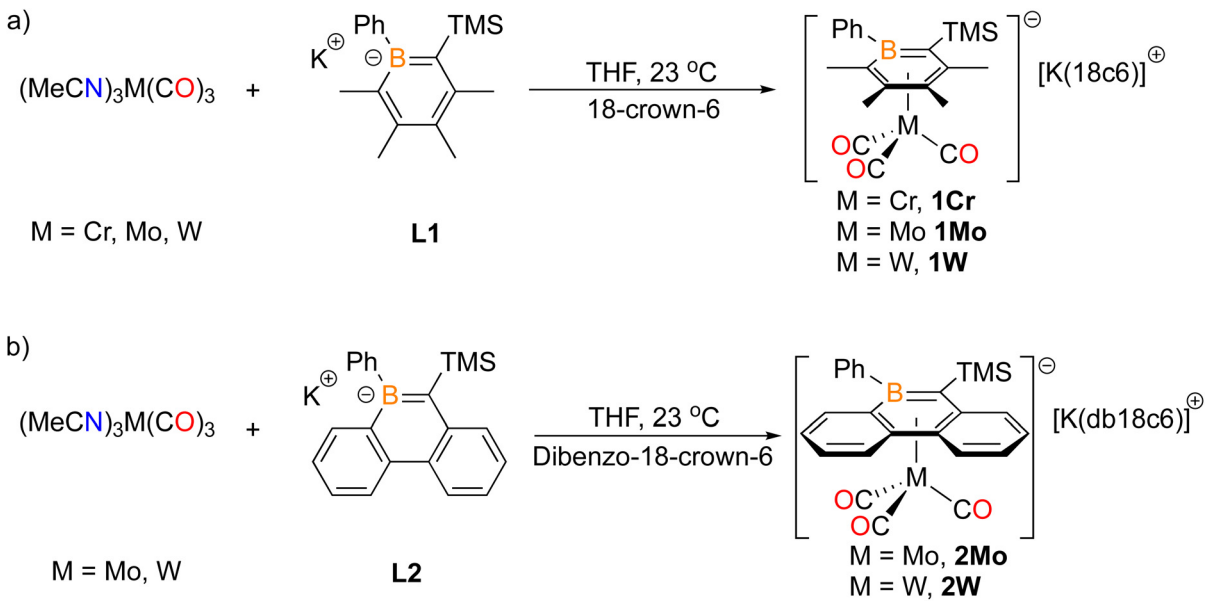


**Scheme 1** Synthesis of group 6 piano-stool complexes with (a) **L1** and (b) **L2** (18c6 = 18-crown-6, db18c6 = dibenzo-18-crown-6).

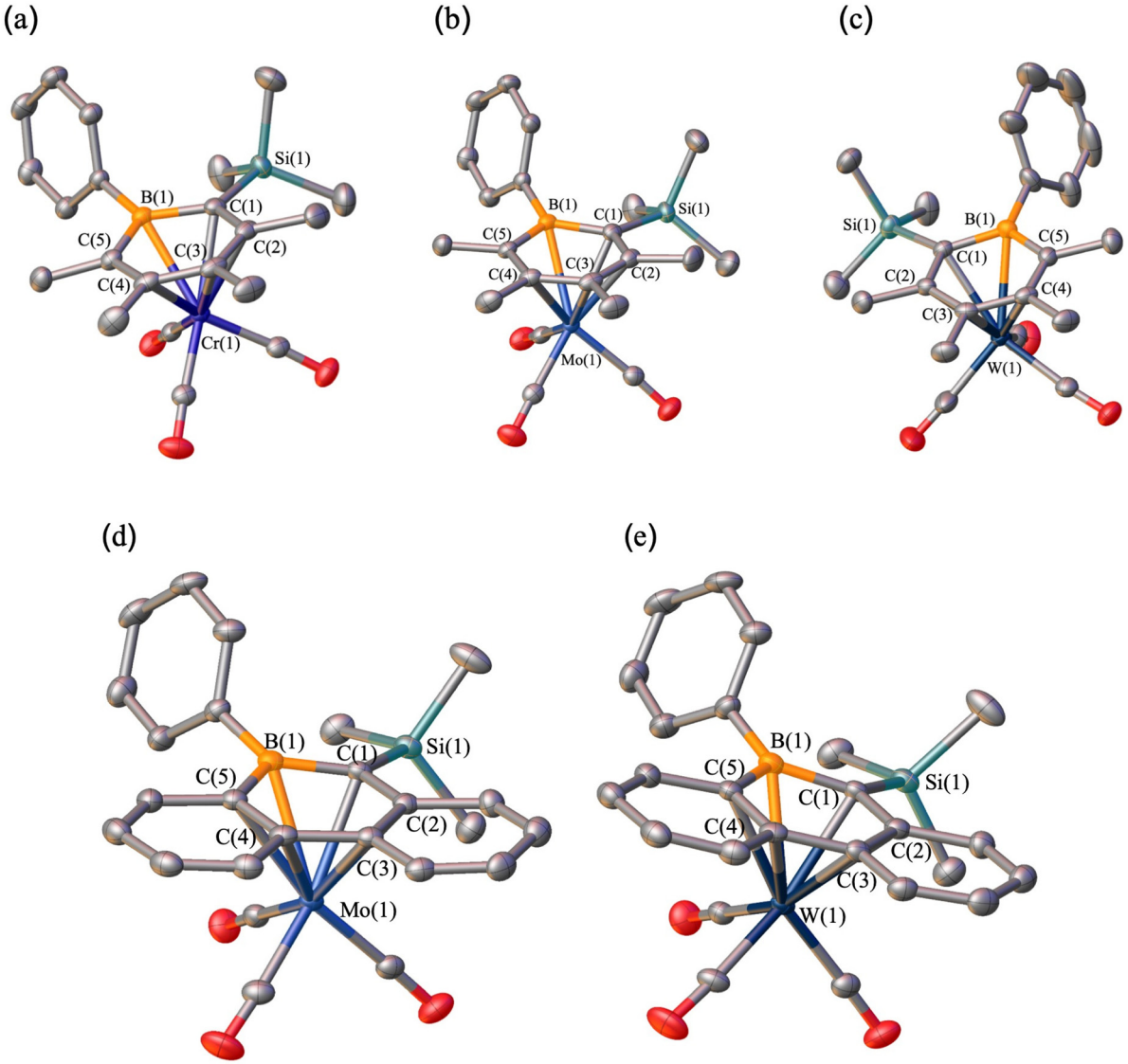


**Fig. 2** Solid-state structures of the anions of (a) **1Cr**, (b) **1Mo**, (c) **1W**, (d) **2Mo** and (e) **2W**. Hydrogen atoms and solvates are omitted for clarity, and thermal ellipsoids are drawn at the 50% probability level. The relevant metrical parameters are presented in Table 1.

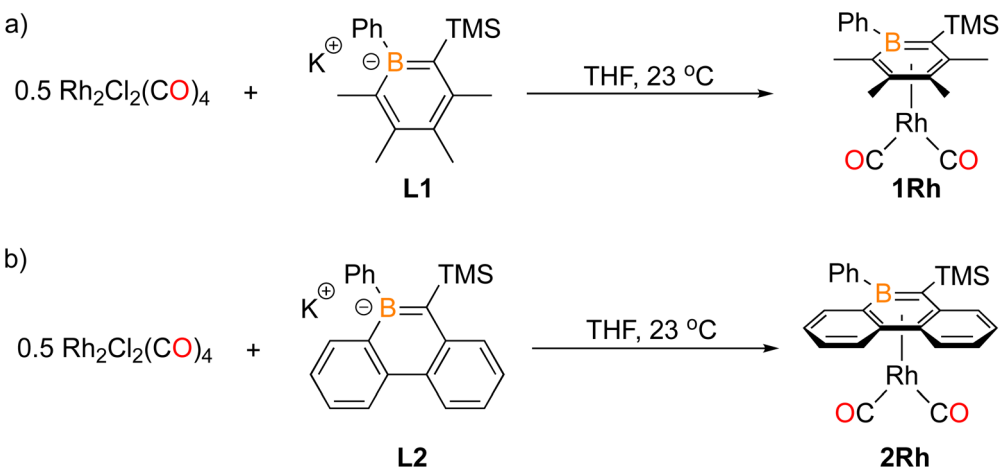


**Scheme 2** Synthesis of (a) **1Rh** and (b) **2Rh**.

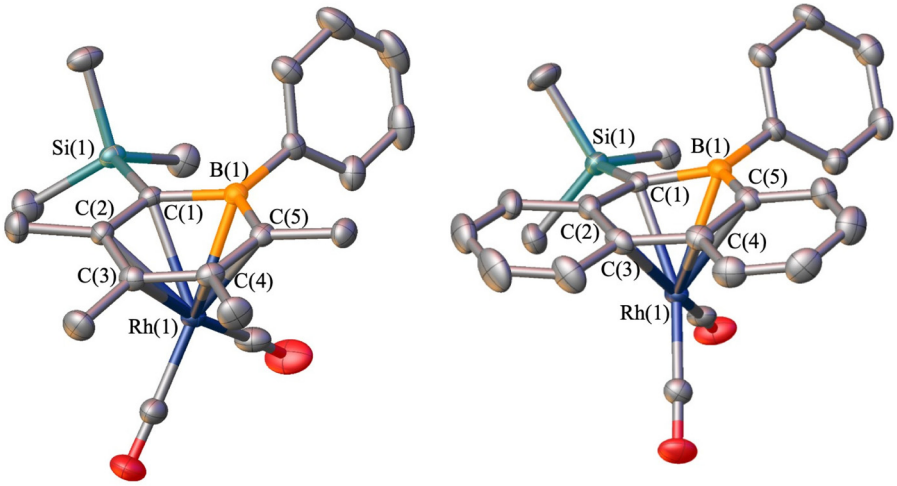


**Fig. 3** Solid-state structures of **1Rh** (left) and **2Rh** (right). Hydrogen atoms and solvates are omitted for clarity, and thermal ellipsoids are drawn at the 50% probability level. Relevant metrical parameters (Å) are in Table 1.

**Table 1** Selected bond lengths and metrical parameters (Å) for the metal carbonyl complexes

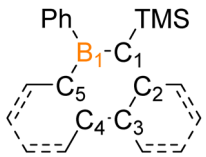


| | 1Cr | 1Mo | 1W | 2Cr[10] | 2Mo | 2W | 1Rh | 2Rh |
|---|---|---|---|---|---|---|---|---|
| B(1)–C(1) | 1.536(3) | 1.539(3) | 1.547(4) | 1.517(5) | 1.517(3) | 1.522(6) | 1.549(2) | 1.538(5) |
| C(1)–C(2) | 1.433(2) | 1.434(3) | 1.427(4) | 1.441(5) | 1.447(3) | 1.452(5) | 1.412(2) | 1.460(5) |
| C(2)–C(3) | 1.427(3) | 1.429(3) | 1.434(4) | 1.449(5) | 1.451(3) | 1.452(6) | 1.446(2) | 1.442(6) |
| C(3)–C(4) | 1.432(3) | 1.435(3) | 1.425(5) | 1.468(5) | 1.468(3) | 1.472(6) | 1.445(2) | 1.483(6) |
| C(4)–C(5) | 1.415(2) | 1.415(3) | 1.423(4) | 1.429(5) | 1.427(3) | 1.432(6) | 1.402(2) | 1.427(5) |
| C(5)–B(1) | 1.524(3) | 1.530(3) | 1.523(4) | 1.546(5) | 1.550(3) | 1.554(6) | 1.542(2) | 1.553(6) |
| B(1)–M | 2.3919(19) | 2.513(2) | 2.474(3) | 2.410(4) | 2.550(3) | 2.537(4) | 2.3803(15) | 2.447(4) |
| C(1)–M | 2.2734(17) | 2.405(2) | 2.408(3) | 2.294(3) | 2.435(2) | 2.420(4) | 2.3379(13) | 2.231(3) |
| C(2)–M | 2.2372(18) | 2.393(2) | 2.397(3) | 2.306(4) | 2.460(2) | 2.445(4) | 2.3533(14) | 2.360(4) |
| C(3)–M | 2.2278(18) | 2.375(2) | 2.356(3) | 2.294(3) | 2.455(2) | 2.445(4) | 2.2070(14) | 2.331(4) |
| C(4)–M | 2.2524(18) | 2.385(2) | 2.378(3) | 2.329(3) | 2.473(2) | 2.458(4) | 2.3480(13) | 2.438(4) |
| C(5)–M | 2.2990(17) | 2.443(2) | 2.422(3) | 2.349(3) | 2.489(2) | 2.483(4) | 2.4132(13) | 2.556(4) |
| M–CO (avg.) | 1.818(2) | 1.942(2) | 1.948(3) | 1.814(4) | 1.933(2) | 1.936(3) | 1.865(2) | 1.867(4) |
| M-ring centroid | 1.752 | 1.927 | 1.911 | 1.805 | 1.990 | 1.971 | 1.826 | 1.884 |
| C–O (avg.) | 1.170(2) | 1.170(3) | 1.168(5) | 1.169(5) | 1.166(3) | 1.171(5) | 1.140(2) | 1.142(5) |
| RMSD | 0.031 | 0.032 | 0.021 | 0.034 | 0.037 | 0.035 | 0.047 | 0.070 |

RMSD = the root-mean-square deviation from planarity of the $BC_5$ ring.

distances for the group 6 complexes are not outside of experimental error to differentiate but fortunately, FT-IR is sensitive for assessing carbonyls.[12]

The FT-IR spectrum for **1W** has overlapping carbonyl bands (appears as two rather than three), while three bands were observed for **1Cr**, **1Mo**, **2Cr**, **2Mo**, and **2W** (Table 2). In all cases, the general trend is that metal complexes with **L2** have higher carbonyl stretching frequencies than **L1**, indicating that **L1** is a stronger donor than **L2**. This is clear in the chromium and molybdenum examples which do not have an overlapping band (**1Cr** $\nu_{co}$ = 1881, 1793, 1766 $cm^{-1}$ *cf.* **2Cr** $\nu_{co}$ = 1903, 1821, 1769 $cm^{-1}$ and **1Mo** $\nu_{co}$ = 1882, 1796, 1767 $cm^{-1}$ *cf.* **2Mo** $\nu_{co}$ = 1910, 1825, 1771 $cm^{-1}$). In the neutral Rh(I) carbonyl complexes, the CO vibration in **L1** complex **1Rh** (2032, 1971 $cm^{-1}$) shows lower stretching frequencies than **2Rh** (2049, 1990 $cm^{-1}$). The CO stretching frequencies of **L1** and **L2** group 6 complexes are significantly lower than the corresponding ($\eta^6$-mesitylene)$M(CO)_3$ complexes.[13] While the complexes with **L1** are generally of lower frequency than the cyclopentadienyl complexes reported in the literature, not all the frequencies are lower than those of the comparison Cp complexes and those with **L2** are very close in value but slightly higher.[6a,14]

Table 2 Experimental FT-IR carbonyl stretching frequencies ($cm^{-1}$). For the Cp complexes, the countercation is sodium

| Metal/ligand | **L1** | **L2** | Cp[6a] | Mesitylene[13] |
|---|---|---|---|---|
| Cr | 1881, 1793, 1766 | 1903, 1821, 1769 | 1897, 1793, 1743 | 1967, 1885 |
| Mo | 1882, 1796, 1767 | 1910, 1825, 1771 | 1899, 1796, 1743 | 1960, 1883 |
| W | 1891, 1773(br)[a] | 1905, 1822, 1768 | 1897, 1792, 1742 | 1956, 1879 |
| Rh | 2032, 1971 | 2049, 1990 | [b] | [b] |

[a] Broad due to two overlapping bands. [b] These complexes are unknown.

Table 3 Computed stretching frequencies ($cm^{-1}$) with a 0.966 scaling factor applied

| Metal/ligand | **L1** | **L2** | Cp | Mesitylene |
|---|---|---|---|---|
| Cr | 1888, 1812, 1762 | 1899, 1816, 1774 | 1895, 1805 | 1971, 1914 |
| Mo | 1892, 1810, 1757 | 1898, 1805, 1772 | 1897, 1801 | 1970, 1906 |
| W | 1884, 1803, 1749 | 1888, 1798, 1763 | 1889, 1794 | 1969, 1904 |
| Rh | 2034, 1985 | 2049, 2000 | 2041, 1987 | 2109, 2067 |

This indicates the following trend in regards to donor strength: **L1** > Cp > **L2** > mesitylene.

Density Functional Theory (DFT) calculations were conducted on the eight complexes as well as the Cp and mesitylene complexes (Table 3 and ESI S57†).[6a,13,15] The calculations were performed using Gaussian 16 at the B3LYP/LANL2DZ level of theory in the gas phase for all the metals and silicon, while the other elements were described using the 6-31+G(d,p) basis set.[16] For the anionic group 6 species, the cations and crown ethers were included. The calculated values with a 0.966 scaling factor applied (which is documented in similar calculations)[17] correlate well with the experimental values and obey the same trends. The group 6 complexes with **L1** and **L2** have three stretching frequencies while the Cp and mesitylene complexes have only two, due to higher symmetry. This makes a direct comparison not possible but in general, the CO stretching frequencies of **L1** bound group 6 complexes are less than those of Cp ligated complexes, with the Cp complexes lower than the **L2** complexes, and the mesitylene group 6 complexes the highest. The DFT studies suggest the same trend in donor strength as the experiments with **L1** being the strongest, then Cp, with **L2** marginally weaker and mesitylene being the weakest.

## Conclusion

The full complement of anionic group 6 piano-stool and neutral rhodium dicarbonyl complexes were accessed by treatment of the potassium salts of substituted boratabenzene (**L1**) or boratraphenanthrene (**L2**) with $M(CO)_3(CH_3CN)_3$ or $Rh_2Cl_2(CO)_4$. X-ray diffraction analysis confirmed $\eta^6$ coordination of the boracyclic ligands to the metal centers with the boratabenzene series more tightly bound to the metal than the boratraphenanthrene series. Experimental and computed $\nu_{co}$ frequencies reveal that **L1** is a stronger donor than **L2** with both being a stronger donor than mesitylene but only **L1** being a stronger donor than cyclopentadiene. This study sheds light on the coordination chemistry of boratabenzene based ligands that could impact the design of new metal complexes.

## Experimental section

### General considerations

All manipulations were performed under an inert atmosphere in a nitrogen-filled MBraun Unilab glove box or using standard Schlenk techniques. Benzene-$d_6$ and $CD_3CN$ for NMR spectroscopy were purchased from Cambridge Isotope Laboratories and dried by stirring for 3 days over $CaH_2$, distilling, and storing over molecular sieves. THF-$d_8$ for NMR spectroscopy was purchased from Cambridge Isotope Laboratories and stored over molecular sieves. All other solvents were purchased from commercial sources as anhydrous grade, dried further using a JC Meyer Solvent System with dual columns packed with solvent-appropriate drying agents, and stored over molecular sieves. Reagents **L1**, **L2**, and tris(acetonitrile)tricarbonylmolybdenum(0) were prepared by the literature procedures.[10,11,18] Tris(acetonitrile)tricarbonylchromium(0) and tris(acetonitrile)tricarbonyltungsten(0) were purchased from Aldrich and used as received. Chlorodicarbonylrhodium (I) dimer was purchased from Strem Chemicals and was also used as received. Multinuclear NMR spectra ($^1H$, $^{13}C\{^1H\}$, $^{11}B$) were recorded on a Bruker Ascend 400 MHz instrument. High resolution mass spectra (HRMS) were obtained at the Baylor University Mass Spectrometry Center on a Thermo Scientific LTQ Orbitrap Discovery spectrometer using ESI or at the University of Texas at Austin Mass Spectrometry Center on a Micromass Autospec Ultima spectrometer using CI. Melting points were measured with a Thomas Hoover Uni-melt capillary melting point apparatus and are uncorrected. FT-IR spectra were recorded on a Bruker Alpha ATR FT-IR spectrometer on solid samples. Single crystal X-ray diffraction data were collected on a Bruker Apex II-CCD detector using Mo-Kα radiation ($\lambda$ = 0.71073 Å). Crystals were selected under paratone oil, mounted on MiTeGen micromounts, and immediately

 

placed in a cold stream of $N_2$. Structures were solved and refined using SHELXTL[19] and figures produced using OLEX2.[20] For the crystal structure of compound **2Rh**, an acetonitrile solvate disordered across a symmetry site was removed using the SQUEEZE function in PLATON.[21]

**1Cr.** A solution of **L1** (58 mg, 0.18 mmol) in THF (1 mL) was added dropwise to a suspension of tris(acetonitrile)tricarbonylchromium (46 mg, 0.18 mmol) in THF (2 mL) while stirring at 23 °C in a vial wrapped in aluminum foil in the dark. After 2 hours, the volatile components were stripped *in vacuo*. The resulting oil was extracted with benzene (2 mL), filtered, and lyophilized to yield a yellow powder. The crude solids were then dissolved in diethyl ether (1 mL), added to solid 18-crown-6 (47 mg, 0.18 mmol), and stirred for an additional 15 minutes. The supernatant was decanted, and the precipitate was washed with 1 mL of benzene and diethyl ether mixed solvent (2 : 1 ratio) to yield **1Cr** as a yellow powder. Yield: 53 mg (41%). d.p. 123 °C. Crystals for X-ray diffraction studies were grown by vapor diffusion of diethyl ether into a benzene solution of **1Cr**. $^1$H NMR (400 MHz, $CD_3CN$): $\delta$ 7.87 (br, 1H, Ar–H), 7.20–7.09 (m, 4H, Ar–H), 3.56 (s, 24H, $CH_2$), 2.24 (s, 3H, $CH_3$), 2.22 (s, 3H, $CH_3$) 2.15 (s, 3H, $CH_3$), 1.49 (s, 3H, $CH_3$), −0.17 (s, 9H, $Si(CH_3)_3$). $^{13}C\{^1H\}$ NMR (101 MHz, $CD_3CN$): $\delta$ 241.93 (CO), 135.21, 126.98, 125.12, 123.85, 119.98, 96.52, 70.92, 24.16, 19.26, 18.55, 17.48, 4.44. $^{11}$B NMR (128 MHz, $CD_3CN$): $\delta$ 27.0. FT-IR ($cm^{-1}$ (ranked intensity)): 2885 (13), 1881 (3), 1793(4) 1766 (1), 1453 (14), 1351 (9), 1308 (15), 1241 (10), 1095 (2), 955 (6), 888 (11), 834 (5), 694 (8), 645 (7), 543 (12). High-resolution mass spectrometry (HRMS) electrospray ionization (ESI): calculated for $C_{21}H_{26}BCrO_3Si$ $[M]^-$, 417.1149; found, 417.1140.

**1Mo.** A solution of **L1** (62 mg, 0.19 mmol) in THF (2 mL) was added dropwise to a suspension of tris(acetonitrile)tricarbonylmolybdenum (58 mg, 0.19 mmol) in THF (2 mL) while stirring at 23 °C in a vial wrapped in aluminum foil in the dark. After 1.5 hours, the volatile components were stripped *in vacuo*. The resulting oil was extracted with diethyl ether (2 mL), added to solid 18-crown-6 (50 mg, 0.19 mmol), and stirred for an additional 15 minutes. The supernatant was decanted, yielding **1Mo** as a pale yellow powder. Yield: 113 mg (78%). d.p. 129 °C. Crystals for X-ray diffraction studies were grown by vapor diffusion of diethyl ether into a benzene solution of **1Mo**. $^1$H NMR (400 MHz, $CD_3CN$): $\delta$ 7.75 (br, 1H, Ar–H), 7.22–7.07 (m, 4H, Ar–H), 3.57 (s, 24H, $CH_2$), 2.34 (s, 3H, $CH_3$), 2.29 (s, 3H, $CH_3$), 2.27 (s, 3H, $CH_3$), 1.57 (s, 3H, $CH_3$), −0.18 (s, 9H, $Si(CH_3)_3$). $^{13}C\{^1H\}$ NMR (101 MHz, $CD_3CN$): $\delta$ 232.41 (CO), 136.00, 134.67, 129.20, 127.10, 125.24, 124.72, 99.87, 70.89, 24.62, 19.67, 18.88, 17.90, 4.79. $^{11}$B NMR (128 MHz, $CD_3CN$): $\delta$ 29.5. FT-IR ($cm^{-1}$ (ranked intensity)): 2883 (13), 1882 (3), 1796 (11), 1767 (1), 1453 (15), 1352 (10), 1241 (9), 1095 (2), 955 (4), 887 (12), 836 (5), 757 (14), 698 (7), 641 (6), 511 (8). High-resolution mass spectrometry (HRMS) electrospray ionization (ESI): calculated for $C_{21}H_{26}BMoO_3Si$ $[M]^-$, 463.0798; found, 463.0775.

**1W.** A solution of **L1** (51 mg, 0.16 mmol) in THF (1 mL) was added dropwise to a suspension of tris(acetonitrile)tricarbonyltungsten (63 mg, 0.16 mmol) in THF (10 mL) while stirring at 23 °C in a vial wrapped in aluminum foil in the dark. After 90 minutes, the volatile components were removed *in vacuo*. The resulting oil was extracted with diethyl ether (3 mL) and added to solid 18-crown-6 (42 mg, 0.16 mmol). The volatile components were immediately stripped *in vacuo*, and the crude solid was extracted with benzene (3 mL), filtered, and lyophilized. The solid power was washed with 1 mL of benzene and diethyl ether mixed solvent (2 : 1 ratio) to yield **1W** as a yellow powder. Yield: 35 mg (26%). d.p. 61 °C. Crystals for X-ray diffraction studies were grown by vapor diffusion of diethyl ether into a benzene solution of **1W**. $^1$H NMR (400 MHz, $CD_3CN$): $\delta$ 7.71 (br, 1H, Ar–H), 7.22–7.08 (m, 4H, Ar–H), 3.57 (s, 24H, $CH_2$), 2.47 (s, 3H, $CH_3$), 2.40 (s, 3H, $CH_3$), 2.31 (s, 3H, $CH_3$). 1.62 (s, 3H, $CH_3$), −0.18 (s, 9H, $Si(CH_3)_3$). $^{13}C\{^1H\}$ NMR (101 MHz, $CD_3CN$): $\delta$ 223.37 (CO), 136.31, 135.11, 127.24, 126.15, 125.40, 121.73, 98.03, 70.89, 24.01, 19.74, 18.91, 17.58, 4.75. $^{11}$B NMR (128 MHz, $CD_3CN$): $\delta$ 28.5. FT-IR ($cm^{-1}$ (ranked intensity)): 2891 (11), 1891 (3), 1773 (2), 1470 (14), 1351 (7), 1242 (8), 1101 (1), 960 (6), 886 (13), 833 (4), 708 (12), 674 (9), 618 (10), 594 (15), 499 (5). High-resolution mass spectrometry (HRMS) electrospray ionization (ESI): calculated for $C_{21}H_{26}BO_3SiW$ $[M]^-$, 549.1254; found, 549.1246.

**2Mo.** A solution of **L2** (87 mg, 0.24 mmol) in THF (2 mL) was added dropwise to a suspension of tris(acetonitrile)tricarbonylmolybdenum (72 mg, 0.24 mmol) in THF (3 mL) while stirring at 23 °C in a vial wrapped in aluminum foil in the dark. After 2 hours, the volatile components were removed *in vacuo*. A solution of dibenzo-18-crown-6 (86 mg, 0.24 mmol) in dichloromethane (4 mL) was added to the resulting solid and stirred for an additional 30 minutes. The reaction mixture was filtered, and the volatile components were evaporated from the filtrate *in vacuo*. The resulting solids were washed with benzene (2 mL) and then subsequently with dichloromethane (1 mL) to give an orange-red powder. Yield: 139 mg (67%). d.p. 139 °C. Crystals for X-ray diffraction studies were grown by vapor diffusion of a dichloromethane solution of **2Mo** into toluene. $^1$H NMR (400 MHz, THF-$d_8$): $\delta$ 8.68 (d, $J$ = 8.0 Hz, 1H, Ar–H), 8.48 (d, $J$ = 8.0 Hz, 1H, Ar–H), 8.33 (br, 1H, Ar–H), 7.89 (d, $J$ = 8.0 Hz, 1H, Ar–H), 7.56 (d, $J$ = 8.0 Hz, 1H, Ar–H), 7.39–7.12 (m, 6H, Ar–H), 7.07 (t, $J$ = 8.0 Hz, 1H, Ar–H), 6.96–6.85 (m, 9H, Ar–H), 4.11 (d, $J$ = 4.0 Hz, 8H, $CH_2$), 3.86 (d, $J$ = 4.0 Hz, 8H, $CH_2$), 0.13 (s, 9H, $Si(CH_3)_3$). $^{13}C\{^1H\}$ NMR (101 MHz, THF-$d_8$): $\delta$ 228.76 (CO), 148.07, 138.67, 136.46, 135.50, 132.48, 128.87, 128.11, 126.96, 126.84, 126.18, 125.38, 123.62, 123.04, 122.22, 120.96, 117.50, 112.31, 102.60, 70.22, 68.26, 4.98. $^{11}$B NMR (128 MHz, THF-$d_8$): $\delta$ 33.2. FT-IR ($cm^{-1}$ (ranked intensity)): 1910 (5), 1825 (12), 1771 (1), 1503 (6), 1453 (10), 1248 (4), 1212 (9), 1120 (3), 1060 (11), 942 (7), 830 (8), 743 (2), 702 (15), 614 (13), 499 (14). High-resolution mass spectrometry (HRMS) electrospray ionization (ESI): calculated for $C_{25}H_{22}BMoO_3Si$ $[M]^-$, 507.0485; found, 507.0471.

**2W.** A solution of **L2** (100 mg, 0.274 mmol) in THF (2 mL) was added dropwise to a solution of tris(acetonitrile)tricarbonyltungsten (107 mg, 0.274 mmol) in THF (8 mL) while stirring at 23 °C in a vial wrapped in aluminum foil in the dark.

After 1.5 hours, dibenzo-18-crown-6 (99 mg, 0.27 mmol) in dichloromethane (4 mL) was added to the reaction mixture, which was stirred for an additional 30 minutes. The volatile components were then evaporated *in vacuo*. The resulting solids were washed with dichloromethane (1 mL) and subsequently with benzene (2 mL) to yield **2W** as a bright red powder. Yield: 103 mg (48%). d.p. 138 °C. Crystals for X-ray diffraction studies were grown by vapor diffusion of a dichloromethane solution of **2W** into toluene. $^{1}$H NMR (400 MHz, THF-$d_8$): $\delta$ 8.57 (d, $J$ = 8.0 Hz, 1H, Ar–H), 8.40 (d, $J$ = 12 Hz, 1H, Ar–H), 8.31 (br, 1H, Ar–H), 7.88 (d, $J$ = 8.0 Hz, 1H, Ar–H), 7.46 (d, $J$ = 8.0 Hz, 1H, Ar–H), 7.35–7.26 (m, 2H, Ar–H), 7.20–7.10 (m, 4H, Ar–H), 7.05 (t, $J$ = 7.2 Hz, 1H, Ar–H), 7.01–6.86 (m, 8H, Ar–H), 6.80 (t, $J$ = 7.4 Hz, 1H, Ar–H), 4.27–4.03 (m, 8H, $CH_2$), 3.96–3.77 (m, 8H, $CH_2$), 0.12 (s, 9H, $Si(CH_3)_3$). $^{13}$C NMR (101 MHz, THF-$d_8$): $\delta$ 218.58 (CO), 147.95, 138.87, 136.86, 135.96, 132.16, 129.16, 129.09, 128.78, 127.62, 127.10, 125.50, 123.67, 123.22, 122.94, 122.22, 121.39, 114.22, 112.13, 99.47, 70.20, 68.16, 4.96. $^{11}$B NMR (128 MHz, THF-$d_8$): $\delta$ 30.8. FT-IR ($cm^{-1}$ (ranked intensity)): 1905 (5), 1822 (9), 1768 (2), 1503 (6), 1453 (11), 1248 (4), 1212 (10), 1120 (3), 1060 (12), 942 (7), 830 (8), 743 (1), 702 (15), 599 (14), 500 (13). High-resolution mass spectrometry (HRMS) electrospray ionization (ESI): calculated for $C_{25}H_{22}BO_3SiW$ $[M]^-$, 593.0941; found, 593.0934.

**1Rh.** A solution of $Rh_2Cl_2(CO)_4$ (22 mg, 0.055 mmol) in THF (1 mL) was added to a solution of **L1** (41 mg, 0.13 mmol) in THF (2 mL) while stirring at 23 °C. After 45 minutes of stirring, the volatile components were evaporated *in vacuo*, and the resulting brown oil was extracted with *n*-pentane (5 mL). The pentane extract was then filtered, and the volatile components were evaporated *in vacuo* from the filtrate to yield **1Rh** as a yellow solid. Yield: 39 mg (81%). d.p. 46 °C. Crystals for X-ray diffraction studies were grown by storing an acetonitrile solution of **1Rh** at −35 °C. $^{1}$H NMR (400 MHz, $C_6D_6$): $\delta$ 7.80–7.45 (br, 2H, Ar–H), 7.33 (t, $J$ = 7.8 Hz, 2H, Ar–H), 7.26–7.19 (m, 1H, Ar–H), 2.05 (s, 3H, $CH_3$), 1.83 (s, 3H, $CH_3$), 1.79 (s, 3H, $CH_3$), 1.78 (s, 3H, $CH_3$), 0.10 (s, 9H, $Si(CH_3)_3$). $^{13}$C{$^{1}$H} NMR (101 MHz, $C_6D_6$): $\delta$ 191.21 (CO), 190.39 (CO), 133.19, 133.15, 127.76, 126.51, 97.70, 97.67, 23.40, 19.58, 18.79, 16.37, 3.23. $^{11}$B NMR (128 MHz, $C_6D_6$): $\delta$ 26.1. FT-IR ($cm^{-1}$ (ranked intensity)): 2032 (5), 1971 (1), 1383 (14), 1295 (15), 1246 (6), 1015 (9), 881 (12), 830 (2), 759 (11), 741 (8), 702 (3), 624 (10), 591 (13), 548 (7), 506 (4). High-resolution mass spectrometry (HRMS) chemical ionization (CI): calculated for $C_{20}H_{26}BO_2RhSi$ $[M]^+$, 440.0850; found, 440.0862.

**2Rh.** A solution of $Rh_2Cl_2(CO)_4$ (26 mg, 0.067 mmol) in THF (2 mL) was added to a solution of **L2** (50 mg, 0.14 mmol) in THF (2 mL) while stirring at 23 °C. After 30 minutes of stirring, the volatile components were evaporated *in vacuo*, and the resulting brown oil was extracted with *n*-pentane (4 mL). The pentane extract was then filtered, and the volatile components were evaporated *in vacuo* from the filtrate to yield **2Rh** as an orange solid. Yield: 57 mg (88%). d.p. 44 °C. Crystals for X-ray diffraction studies were grown by storing an acetonitrile solution of **2Rh** at −35 °C. $^{1}$H NMR (400 MHz, $C_6D_6$): $\delta$ 8.12–8.08 (m, 1H, Ar–H), 7.83–7.71 (m, 4H, Ar–H), 7.68 (d, $J$ = 8.0 Hz, 1H, Ar–H), 7.39 (t, $J$ = 8.0 Hz, 2H, Ar–H), 7.33–7.30 (m, 1H, Ar–H), 7.26–7.22 (m, 1H, Ar–H), 7.13–7.09 (m, 2H, Ar–H), 7.02 (t, $J$ = 7.5 Hz, 1H, Ar–H), 0.29 (s, 9H, $Si(CH_3)_3$). $^{13}$C{$^{1}$H} NMR (101 MHz, $C_6D_6$): $\delta$ 134.85, 132.18, 129.96, 129.95, 128.77, 128.73, 128.66, 127.71, 127.31, 127.10, 126.99, 122.09, 118.25, 118.24, 99.89, 99.87, 3.01. $^{11}$B NMR (128 MHz, $C_6D_6$): $\delta$ 35.1. FT-IR ($cm^{-1}$ (ranked intensity)): 2049 (2), 1990 (1), 1427 (11), 1249 (5), 927 (10), 832 (3), 745 (4), 721 (13), 702 (7), 612 (8), 593 (14), 580 (15), 549 (6), 492 (9), 423 (12). High-resolution mass spectrometry (HRMS) chemical ionization (CI): calculated for $C_{24}H_{22}BO_2RhSi$ $[M]^+$, 484.0537; found, 484.0533.

## Author contributions

The manuscript was written through contributions of all authors. All authors have given approval to the final version of the manuscript.

## Conflicts of interest

The authors declare no competing financial interest.

## Acknowledgements

We are grateful to the Welch Foundation (Grant No. AA-1846) and the National Science Foundation (Award No. 1753025) for their generous support of this work.

## References

1 G. E. Herberich, G. Greiss and H. F. Heil, *Angew. Chem., Int. Ed. Engl.*, 1970, **9**, 805–806.
2 (*a*) A. J. Ashe and P. Shu, *J. Am. Chem. Soc.*, 1971, **93**, 1804–1805; (*b*) G. E. Herberich and H. Ohst, in *Adv. Organomet. Chem.*, ed. F. G. A. Stone and R. West, Academic Press, 1986, vol. 25, pp. 199–236; (*c*) A. Mushtaq, W. Bi, M.-A. Légaré and F.-G. Fontaine, *Organometallics*, 2014, **33**, 3173–3181; (*d*) S. Qiao, D. A. Hoic and G. C. Fu, *J. Am. Chem. Soc.*, 1996, **118**, 6329–6330; (*e*) J. S. Rogers, R. J. Lachicotte and G. C. Bazan, *J. Am. Chem. Soc.*, 1999, **121**, 1288–1298; (*f*) G. C. Fu, in *Adv. Organomet. Chem.*, Academic Press, 2001, vol. 47, pp. 101–119.
3 (*a*) M. C. Amendola, K. E. Stockman, D. A. Hoic, W. M. Davis and G. C. Fu, *Angew. Chem., Int. Ed. Engl.*, 1997, **36**, 267–269; (*b*) J. T. Goettel and H. Braunschweig, *Coord. Chem. Rev.*, 2019, **380**, 184–200.
4 (*a*) A. J. Ashe, S. Al-Ahmad and X. Fang, *J. Organomet. Chem.*, 1999, **581**, 92–97; (*b*) P. Cui and Y. Chen, *Coord. Chem. Rev.*, 2016, **314**, 2–13; (*c*) A. J. Ashe, S. Al-Ahmad, X. Fang and J. W. Kampf, *Organometallics*, 1998, **17**, 3883–3888; (*d*) M. Davidson, A. K. Hughes, K. Wade and T. Marder, *Contemporary boron chemistry*, Royal Society of Chemistry, 2000; (*e*) Y.-S. Meng, C.-H. Wang, Y.-Q. Zhang,

 

X.-B. Leng, B.-W. Wang, Y.-F. Chen and S. Gao, *Inorg. Chem. Front.*, 2016, **3**, 828–835; (*f*) G. C. Bazan, G. Rodriguez, A. J. Ashe, S. Al-Ahmad and J. W. Kampf, *Organometallics*, 1997, **16**, 2492–2494; (*g*) J. Tweddell, D. A. Hoic and G. C. Fu, *J. Org. Chem.*, 1997, **62**, 8286–8287; (*h*) G. E. Herberich, U. Englert, B. Ganter, M. Pons and R. Wang, *Organometallics*, 1999, **18**, 3406–3413; (*i*) D. H. Woodmansee, X. Bu and G. C. Bazan, *Chem. Commun.*, 2001, 619–620; (*j*) C. Wang, X. Leng and Y. Chen, *Organometallics*, 2015, **34**, 3216–3221; (*k*) V. Perez, P. Audet, W. Bi and F.-G. Fontaine, *Dalton Trans.*, 2016, **45**, 2130–2137.

5 (*a*) M. Zhou, L. Andrews and C. W. Bauschlicher, *Chem. Rev.*, 2001, **101**, 1931–1962; (*b*) A. M. Ricks, Z. D. Reed and M. A. Duncan, *J. Am. Chem. Soc.*, 2009, **131**, 9176–9177; (*c*) F. Aubke and C. Wang, *Coord. Chem. Rev.*, 1994, **137**, 483–524; (*d*) A. W. Ehlers, S. Dapprich, S. F. Vyboishchikov and G. Frenking, *Organometallics*, 1996, **15**, 105–117; (*e*) R. H. Crabtree, *The organometallic chemistry of the transition metals*, John Wiley & Sons, 2009.

6 (*a*) M. Y. Darensbourg, P. Jimenez, J. R. Sackett, J. M. Hanckel and R. L. Kump, *J. Am. Chem. Soc.*, 1982, **104**, 1521–1530; (*b*) D. A. Brown and F. J. Hughes, *J. Chem. Soc. A*, 1968, 1519–1523; (*c*) M. J. Aroney, R. M. Clarkson, R. J. Klepetko, A. F. Masters and R. K. Pierens, *J. Organomet. Chem.*, 1990, **393**, 371–378; (*d*) A. D. Hunter, V. Mozol and S. D. Tsai, *Organometallics*, 1992, **11**, 2251–2262; (*e*) E. R. Davidson, K. L. Kunze, F. B. C. Machado and S. J. Chakravorty, *Acc. Chem. Res.*, 1993, **26**, 628–635; (*f*) J. M. Oh, S. J. Geib and N. J. Cooper, *Acta Crystallogr., Sect. C: Cryst. Struct. Commun.*, 1998, **54**, 581–583; (*g*) M. Rosillo, G. Domínguez and J. Pérez-Castells, *Chem. Soc. Rev.*, 2007, **36**, 1589–1604; (*h*) G. Bistoni, S. Rampino, N. Scafuri, G. Ciancaleoni, D. Zuccaccia, L. Belpassi and F. Tarantelli, *Chem. Sci.*, 2016, **7**, 1174–1184; (*i*) D. Koch, Y. Chen, P. Golub and S. Manzhos, *Phys. Chem. Chem. Phys.*, 2019, **21**, 20814–20821.

7 G. E. Herberich and D. Söhnen, *J. Organomet. Chem.*, 1983, **254**, 143–147.

8 V. Pérez, S. S. Barnes and F.-G. Fontaine, *Eur. J. Inorg. Chem.*, 2014, **2014**, 5698–5702.

9 (*a*) H.-B. Burgi, A. Raselli, D. Braga and F. Grepioni, *Acta Crystallogr., Sect. B: Struct. Sci.*, 1992, **48**, 428–437; (*b*) Z. Y. Own, S. M. Wang, J. F. Chung, D. W. Miller and P. P. Fu, *Inorg. Chem.*, 1993, **32**, 152–159.

10 T. A. Bartholome, A. Kaur, D. J. D. Wilson, J. L. Dutton and C. D. Martin, *Angew. Chem., Int. Ed.*, 2020, **59**, 11470–11476.

11 (*a*) G. K. Wisofsky, K. Rojales, X. Su, T. A. Bartholome, A. Molino, A. Kaur, D. J. D. Wilson, J. L. Dutton and C. D. Martin, *Inorg. Chem.*, 2021, **60**, 18981–18989; (*b*) T. A. Bartholome, K. R. Bluer and C. D. Martin, *Dalton Trans.*, 2019, **48**, 6319–6322.

12 L. E. Orgel, *Inorg. Chem.*, 1962, **1**, 25–29.

13 R. S. Armstrong, M. J. Aroney, C. M. Barnes and K. W. Nugent, *Appl. Organomet. Chem.*, 1990, **4**, 569–580.

14 U. Behrens and F. Edelmann, *J. Organomet. Chem.*, 1984, **263**, 179–182.

15 F. Mazzotta, K. W. Törnroos and D. Kunz, *Organometallics*, 2020, **39**, 3590–3601.

16 (*a*) Y. Sert, H. S. Clayton, H. Gökce and K. C. Tapala, *J. Mol. Struct.*, 2019, **1188**, 86–98; (*b*) M. J. Frisch, G. W. Trucks, H. B. Schlegel, G. E. Scuseria, M. A. Robb, J. R. Cheeseman, G. Scalmani, V. Barone, G. A. Petersson, H. Nakatsuji, X. Li, M. Caricato, A. V. Marenich, J. Bloino, B. G. Janesko, R. Gomperts, B. Mennucci, H. P. Hratchian, J. V. Ortiz, A. F. Izmaylov, J. L. Sonnenberg, D. Williams-Young, F. Ding, F. Lipparini, F. Egidi, J. Goings, B. Peng, A. Petrone, T. Henderson, D. Ranasinghe, V. G. Zakrzewski, J. Gao, N. Rega, G. Zheng, W. Liang, M. Hada, M. Ehara, K. Toyota, R. Fukuda, J. Hasegawa, M. Ishida, T. Nakajima, Y. Honda, O. Kitao, H. Nakai, T. Vreven, K. Throssell, J. A. Montgomery Jr., J. E. Peralta, F. Ogliaro, M. J. Bearpark, J. J. Heyd, E. N. Brothers, K. N. Kudin, V. N. Staroverov, T. A. Keith, R. Kobayashi, J. Normand, K. Raghavachari, A. P. Rendell, J. C. Burant, S. S. Iyengar, J. Tomasi, M. Cossi, J. M. Millam, M. Klene, C. Adamo, R. Cammi, J. W. Ochterski, R. L. Martin, K. Morokuma, O. Farkas, J. B. Foresman and D. J. Fox, Gaussian 16, Revision C.01, Gaussian, Inc., Wallingford CT, 2016.

17 (*a*) M. K. Assefa, J. L. Devera, A. D. Brathwaite, J. D. Mosley and M. A. Duncan, *Chem. Phys. Lett.*, 2015, **640**, 175–179; (*b*) S. Fernández-Moyano, M. N. Peñas-Defrutos, C. Bartolomé and P. Espinet, *Inorg. Chem.*, 2021, **60**, 14410–14417.

18 D. P. Tate, W. R. Knipple and J. M. Augl, *Inorg. Chem.*, 1962, **1**, 433–434.

19 G. Sheldrick, *Acta Crystallogr., Sect. A: Found. Crystallogr.*, 2008, **64**, 112–122.

20 O. V. Dolomanov, L. J. Bourhis, R. J. Gildea, J. A. K. Howard and H. Puschmann, *J. Appl. Crystallogr.*, 2009, **42**, 339–341.

21 A. Spek, *J. Appl. Crystallogr.*, 2003, **36**, 7–13.